International Journal of Civil Engineering and Technology (IJCIET)
Volume 10, Issue 03, March 2019, pp. 403–412, Article ID: IJCIET_10_03_041
Available online at http://www.iaeme.com/ijmet/issues.asp?JType=IJCIET&VType=10&IType=3
ISSN Print: 0976-6308 and ISSN Online: 0976-6316

DEEP PERCOLATION CHARACTERTISTICS VIA SOIL MOISTURE SENSOR APPROACH IN SAIGON RIVER BASIN, VIETNAM

Tran Thanh Long
Ph.D Student, Department of Water Resources Engineering,
Faculty of Engineering, Chulalongkorn University, Bangkok, Thailand

Sucharit Koontanakulvong
Associate Professor, Department of Water Resources Engineering,
Faculty of Engineering, Chulalongkorn University, Bangkok, Thailand

ABSTRACT

As a critical factor of the groundwater balance, the deeper percolation rate plays an essential role in determining sustainable yields for groundwater resources, especially in water managements for consecutive drought years. Although, there are many methods to estimate deeper percolation, investigation of deeper percolation somehow remains a challenging task.–Hence, the paper focused on to explore deep percolation characteristics of three soil type utilizing Richard's function (Hydrus 1D) and observed soil moisture via field moisture sensors. The maximum deep percolation rate of sand clay loam, sand clay, and clay are estimated to be 4.5 mm/day, 3.5 mm/day, and 2.4 mm/day, respectively. The annual percolation ratios of sand clay loam, sand clay, and clay are 0.34, 0.27 and 0.04, respectively. The average monthly percolation rates of sand clay loam, sand clay, and clay vary 2-4.5 mm/day, 1.5-3.5 mm/day, and 0.5-2 mm/day, respectively with the rainfall intensity of 4-14 mm/day. The experiment gave an insight on deeper percolation characteristics as well as potential land recharge from rainfall utilizing soil moisture approach for future groundwater balance evaluation.

Key words: Deep percolation; Hydrus 1D; soil moisture, sensor, Saigon River basin.

Cite this Article: Tran Thanh Long, Sucharit Koontanakulvong, Deep Percolation Charactertistics Via Soil Moisture Sensor Approach in Saigon River Basin, Vietnam, *International Journal of Civil Engineering and Technology* 10(3), 2019, pp. 403–412.
http://www.iaeme.com/IJCIET/issues.asp?JType=IJCIET&VType=10&IType=3

1. INTRODUCTION

Although land recharge is one of important factor as river recharge for sustainable groundwater management [1, 2], though investigation of land recharge somehow remains a challenging task. Since 1960s, there are varied commonly methods applied to estimate natural groundwater recharge, e.g., i) soil water balance method [3-6], ii) zero flux plane method [7, 8], iii) one-dimensional soil water flow model [9-11]; iv) infiltration test using single ring, double rings, the well permeameter [12, 13], v) inverse modeling technique [14-16], vi) ground water level fluctuation method [5, 17, 18], vii) Chemical/ radioactive method [19, 20]. However, these methods sometime are difficult and expensive in the field test. Moreover, the water balance in unsaturated zone cannot be evaluated easily and lead incorrectly equated with the sustainable yield of an aquifer. Along the development of technology, soil water content can be monitored via Arduino soil moisture sensor [21]. This approach shows potential useful to validate soil profile under water movement process. Hence, the aim of the paper is to explore deep percolation characteristics of three soil types utilizing Richard's function (Hydrus 1D) and observed soil moisture via field sensors. First, the field measurement system was designed and installed in three locations in the Saigon Basin, Vietnam. Second, the daily deep percolations of 3 soil types (sand clay loam, sand clay, and clay) were simulated using the Hydrus 1D model. The water retention parameters were calibrated and verified from Oct 2017 to Dec 2018 by field experimental data in the study area. Third, relationships of effective rainfall and deep percolation were analyzed to detect the deep percolation functions for 3 soil types in the study area by simulated results from Apr 2017 to Dec 2018. These investigations gave an insight on deeper percolation characteristics as well as potential land recharge from rainfall utilizing soil moisture approach for developing groundwater modeling to evaluate groundwater balance in the future.

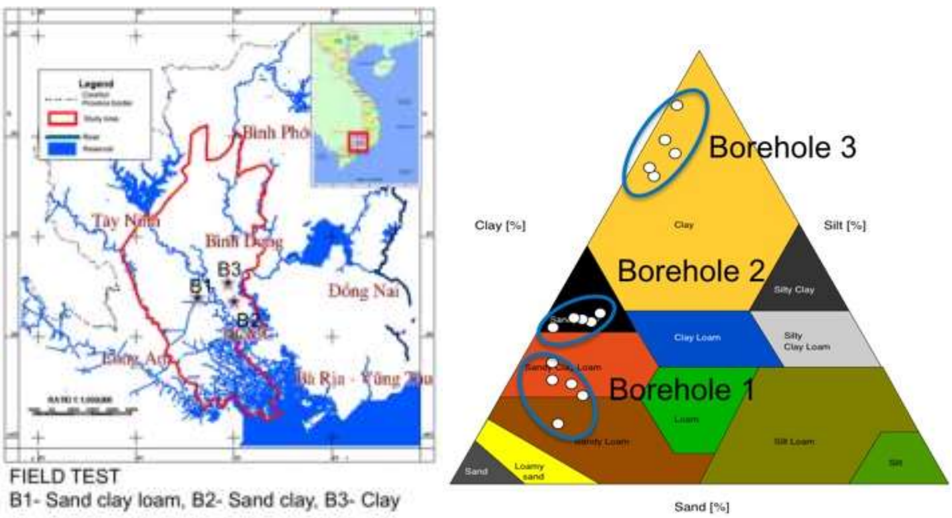

Figure 1 Study area field measurement area

2. MATERIALS AND METHODS

The study was conducted by installing soil moisture sensors in 3 field sites with automatic data collection. These soil samples were collected to calibrate with soil moisture sensors in the lab. Then, the percolation flows were simulated using Richard's function (Hydrus 1D). The water retention parameters were estimated by inverse modeling utilizing observed soil moisture in the field. The performance of soil moisture simulation is justified due to statistic parameters and the regression. Finally, the functions of percolation rate with effective rainfall (rainfall – evapotranspiration), rainfall intensity (rainfall/no of days), percolation rate (percolation/effective rainfall) of three soil types were determined. The procedures of study are shown as Figure 2.

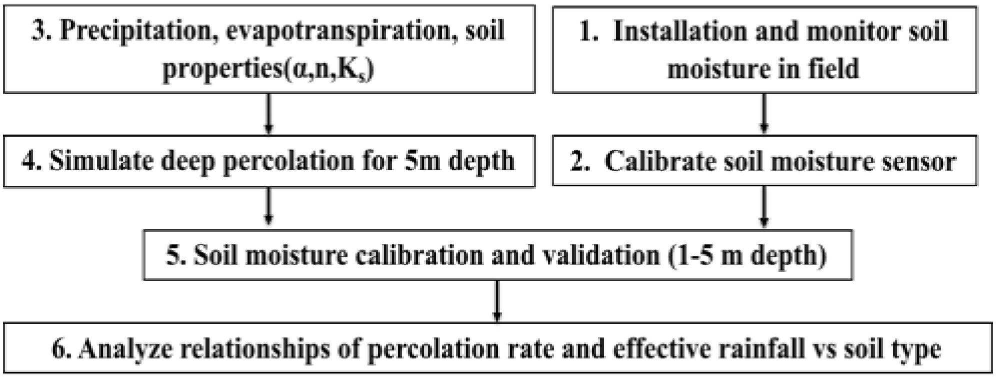

Figure 2 Study procedures

2.1. Field installation and measurement

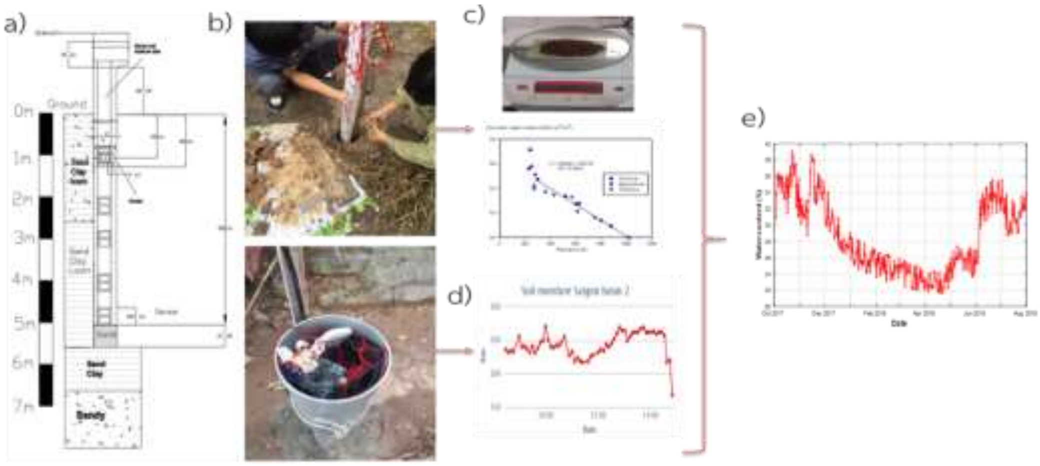

Figure 3 Approach of field installation and measurement (a: bore-log design; b: inject sensor into soil; c: calibration soil moisture; d: field measurement data; e: monitor soil moisture)

The motivation of soil moisture sensor in this paper is adapted from low-cost soil moisture profile probe [21]. The soil moisture sensor developed includes 2 parts: sensing parts and reading board. First, the copper sensing part consisted of two wide bars, with a width and length of 25 and 55 mm, respectively. There was a 1 mm gap between the two bars. These two bars work as a resistor. The wiring part extended to the end of the copper plate and was connected to a soil moisture module. Then, the soil moisture sensing parts and wiring are attached to the aluminium bar. The circuit includes five soil moisture sensing parts to measure the electrical resistance of soil at 1m, 2m, 3m, 4m, and 5m. Second, to measure the soil moisture, Arduino board, which is an open-source electronics platform, is utilized during field measurement. The reader board consists of soil moisture module and Lambda board. The soil moisture module measures the soil resistance, while the Lambda board records the data hourly. The power is supplied from USB 5v 1A. The data was recorded in cloud and downloaded weekly. The soil moisture of each soil type is calibrated with moisture measurement in the lab. Then, the measurements in three field sites are converted to soil moisture. The soil moisture approach is summarized and shown in Figure 3.

2.2. Theories used

The governing flow equation for the uniform Darcian flow of water in a porous medium is adopted by the following modified form of the Richards' equation: [22]

$$\frac{\delta\theta}{\delta t} = \frac{\delta}{\delta x_i}\left[K\left(K_{ij}^{A}\frac{\delta h}{\delta x_j} + K_{iz}^{A}\right)\right] - S \quad (1)$$

Where θ is the volumetric water content, (m^3m^{-3}), K is the hydraulic conductivity (mm/day), h is the pressures head (mm) , S is a sink term (1/day), $x_{i(i-1,2)}$ are the spatial coordinates [L], t is the time (day), z is the vertical ordinate (mm), $K^A{}_{ij}$ are components of a dimensionless anisotropy tensor K^A. K is the unsaturated hydraulic conductivity function (mm/day) given by

$$K(h) = K_s S_e^{\frac{1}{2}}\left[1 - \left(1 - S_e^{\frac{1}{m}}\right)^m\right]^2 \quad (2)$$

$$\theta(h) = \begin{cases} \theta_r + \dfrac{\theta_s - \theta_r}{[1 - |\alpha h|^n]^m} & h < 0 \\ \theta_s & h \geq 0 \end{cases} \quad (3)$$

$$S_e = \frac{\theta - \theta_r}{\theta_s - \theta_r} \quad (4)$$

$$m = 1 - \frac{1}{n}, \quad n > 1 \quad (5)$$

Where S_e is the effective water content, θ_r denote the residual water content, θs denote the saturated water content, K_s is the saturated hydraulic conductivity (mm/day), α is the inverse of the air-entry value (or bubbling pressure), n is a pore-size distribution index.

The x-components of the percolation rate are computed for each node N according to [22]

$$q_N^{j+1} = -K_{N-\frac{1}{2}}^{j+1}\left(\frac{h_N^{j+1} - h_{N-1}^{j+1}}{\Delta x_{N-1}} + 1\right) - \frac{\Delta x_{N-1}}{2}\left(\frac{\theta_N^{j+1} - \theta_N^{j}}{\Delta t} + S_N^j\right) \quad (6)$$

Where θ is the volumetric water content, (m^3m^{-3}), Δt is time calculation (d), Δx is grid size (mm), j is time step, N indicate the position node in the finite difference mesh.

The data of percolation, evaporation, and observed water content of study area were recorded from Oct 2017 to Dec 2018 though the simulation was run from Apr 2017 to Dec 2018. The upper boundary condition is set as atmosphere condition. The bottom boundary condition is set as seepage condition (as shown in Figure 4). The initial retentions parameters (θ_r, θ_s, α , n, K_s) are referred from Rosetta program [23].

3. RESULTS

From the field sensor measurement, soil moisture movements of 3 soil types in wetting and drying phases are shown in Figure 3. The movement of soil moisture in sand clay loam is the highest. Clay shows the lowest movement in soil moisture. The soil moisture increases after rainy season and decrease after dry season. The measurement data show that installed soil moisture sensors gave reliable values under natural field conditions. Then, the analysis relationship between percolation rate and effective rainfall of three soil type can apply the field soil moisture data via installed sensors.

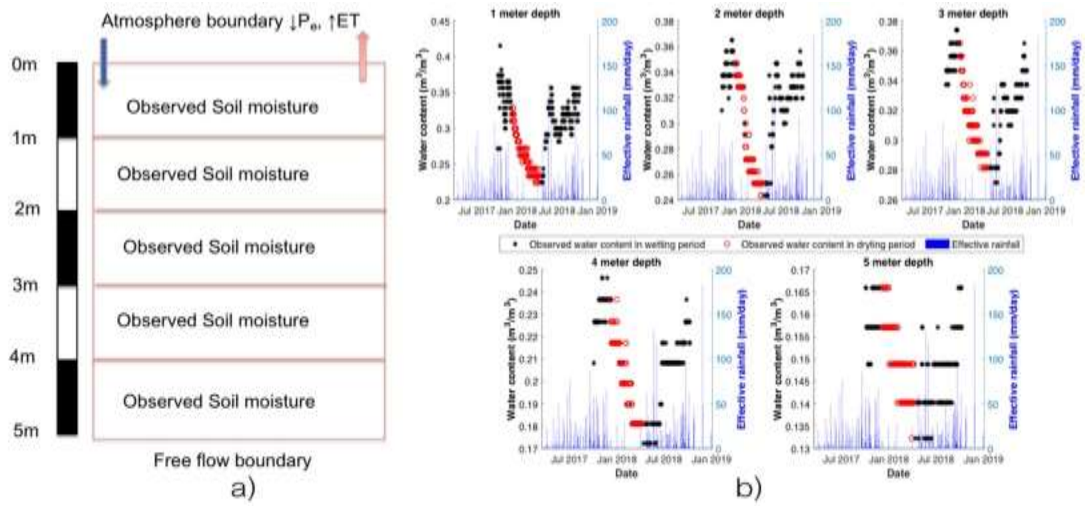

Figure 4 Field soil moisture measurement (a. boundary conditions from field measurement; b. measured soil moisture and effective rainfall)

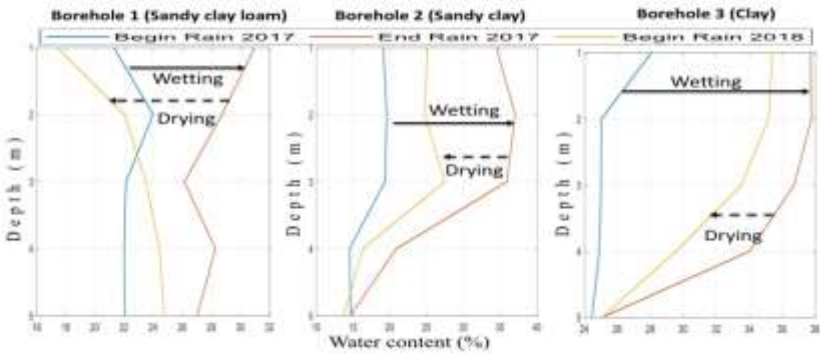

Figure 5 Soil moisture movements of 3 soil types at rainy season and dry season 2017

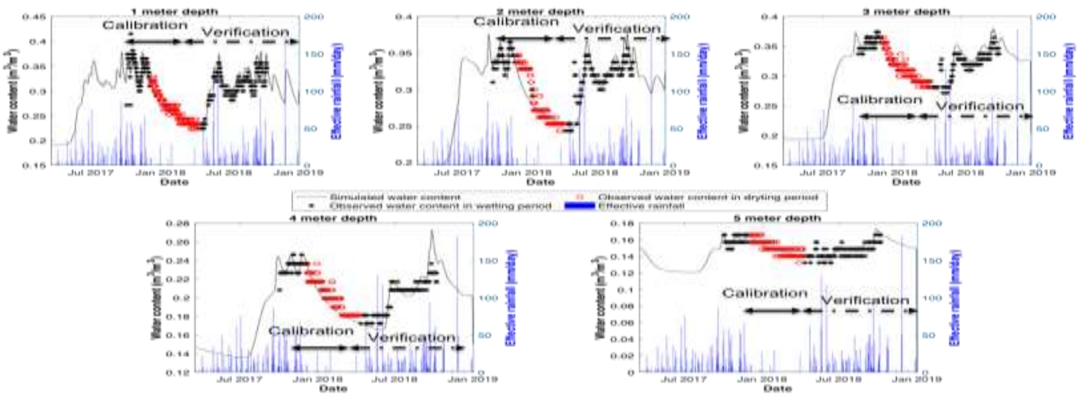

Figure 6 Calibration and verification soil moisture model of sand clay

Retention parameter calibrations relied on performance statistics of observed soil moisture. In calibration step, the calculated soil moistures of three soil type match well with observed data (as an example in Figure 6). The maximum error (%) is 2.98 to 1.45. The minimum error (%) is 0. The mean error (%) is 0.3 to 1.5. The RMSE is 0.4 to 1.8. The R-square is 0.64 to 0.912. In verification step, the calculated soil moistures of three soil type are closed with observed data. The maximum error (%) is 4.68 to 1.35. The minimum error (%) is 0. The mean error (%) is 0.4 to 1.1. The RMSE is 0.5 to 1.2. The R-square is 0.66 to 0.94 as shown in Table 1.

Table 1 Statistic parameters of soil moisture's calibration and verification

Soil type	Period	Calibration			Verification		
		Mean Error	RMSE	R^2	Mean Error	RMSE	R^2
Sand clay loam	Dry	1.4	1.5	0.806	1	1.1	0.852
	Wet	1.5	1.8	0.912	1	1.2	0.940
Sand clay	Dry	1.0	1.2	0.706	0.5	0.6	0.660
	Wet	0.8	1.2	0.874	1.1	1.3	0.806
Clay	Dry	0.3	0.4	0.642	0.5	0.6	0.608
	Wet	0.4	0.5	0.658	0.4	0.5	0.612

Table 2 shows the soil retention parameter values after calibration and verification. The soil retention parameters are proportional with percentage of sand. The α, n, K parameters decrease in deeper depths. The sand clay loam has highest hydraulic conductivity. The lowest hydraulic conductivity is clay. In addition, the parameters of sand clay and clay showed agreement with defaulted values from Hydrus1-D [23]. However, the hydraulic conductivity of sand clay loam is lower than the defaulted value due to the higher silt ratio in the soil sample than referred value.

Table 2 Soil retention parameters after calibration and verification

	Depth (m)	0-1	1-2	2-3	3-4	4-5	defaulted in Hydrus 1-D
Sand clay loam	θ_r	0.065	0.061	0.061	0.06	0.06	0.065
	θ_s	0.41	0.38	0.38	0.39	0.38	0.39
	α (1/mm)	0.0075	0.0029	0.00277	0.0029	0.0025	0.0059
	n(-)	1.89	1.6	1.64	1.48	1.7	1.48
	K(mm/day)	361	124.4	120.3	114	120	314
Sand clay	θ_r	0.1	0.1	0.1	0.1	0.1	0.1
	θ_s	0.38	0.38	0.38	0.38	0.38	0.38
	α (1/mm)	0.0035	0.0032	0.0031	0.0027	0.00015	0.0027
	n(-)	1.65	1.62	1.65	2.2	2.1	1.23
	K(mm/day)	55.8	51	45	60	65	51
Clay	θ_r	0.068	0.068	0.068	0.068	0.068	0.065
	θ_s	0.39	0.39	0.39	0.385	0.385	0.41
	α (1/mm)	0.0015	0.0012	0.0008	0.0006	0.0004	0.0008
	n(-)	1.29	1.25	1.25	1.26	1.75	1.09
	K(mm/day)	15.6	17.6	18.1	24	27	28

Figure 7 demonstrates the hysteretic soil-water retention curves (SWRC) of three soil types at the depths of 1, 5 m from soil surface. The results illustrated good fitting shape of the unsaturated hydraulic conductivity function near saturation. Moreover, the simulations show that hysteresis of percolation rate between drying phase and wetting phase relies on void space and pore size distribution, which are in agreement with experimental results from Yang, 2004 [24]. In example, with the lowest pore-size index, water is difficult to pass through clay, which cause large hysteresis for clay soil (as in Table 2). In addition, the percolation fluxes decrease in each soil depth due to the evapotranspiration influence at soil surface.

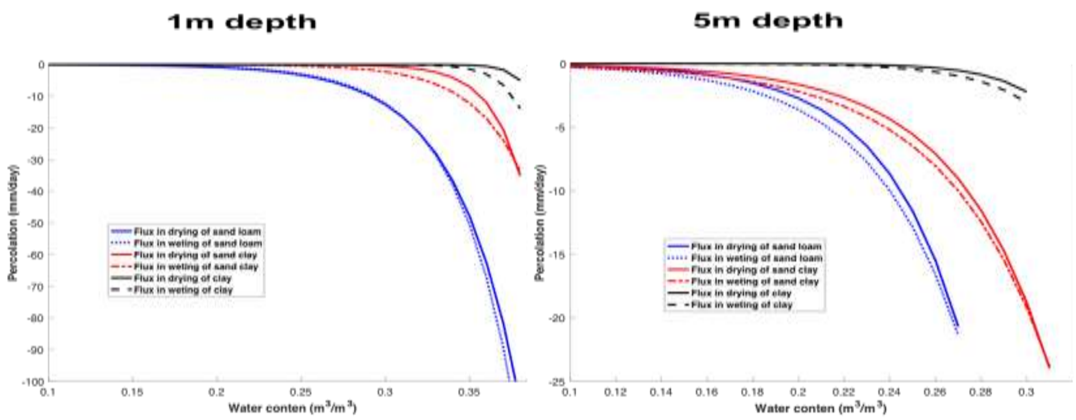

Figure 7 The hysteretic soil-water retention curves (SWRC) of three soil types at 1m and 5m

The average monthly percolation rates of three soil type pattern correspond to effective rainfall. The deep percolations proceed mainly in wet period, while dry period gave very low percolation (as an example in Figure 8). The percolation rate at 5 meter depth is in range 0-4 mm/day. Table 3 shows average percolation rates of three soil type in dry and wet periods of 2017-2018. Due to the permeability property of soil, the derived percolation rate in fluxes in deeper depth are lower than in upper depth of each soil type in the study area. The amount percolation is the highest for sand clay loam and the lowest for clay. The experiment data are in accordance with the percolation rate of sand clay loam (2.3 mm/day) in Phitsanulok, Thailand [25, 26].

Table 3 Average percolation rates of 3 soil types in dry and wet periods of 2017-2018

Soil type	Period	Wet 2017	Dry 2017	Wet 2018	Dry 2018	Annual 2017 - 2018
	Days	238	146	251	30	384
	Effective rainfall (mm)	1651.72	143.08	1872.46	56.4	1794.8
	Rainfall intensity (mm/day)	6.94	0.98	7.46	1.88	4.67
Sand clay loam	Percolation rate 1m (mm/day)	5.37	0.47	5.71	0.25	3.51
	Percolation rate 2m (mm/day)	4.46	0.31	4.55	0.22	2.88
	Percolation rate 3m (mm/day)	4.05	0.24	4.08	0.22	2.6
	Percolation rate 4m (mm/day)	2.97	0.15	3.3	0.18	1.9
	Percolation rate 5m (mm/day)	2.51	0.11	2.73	0.19	1.6
	Percolation ratio (-)	0.36	0.11	0.37	0.1	0.34
Sand clay	Percolation rate 1m (mm/day)	5.27	0.25	5.17	0.29	3.36
	Percolation rate 2m (mm/day)	4.33	0.2	4.87	0.25	2.76
	Percolation rate 3m (mm/day)	4.26	0.17	4.5	0.2	2.7
	Percolation rate 4m (mm/day)	3.01	0.13	3.12	0.17	1.92
	Percolation rate 5m (mm/day)	1.95	0.1	2.26	0.15	1.25
	Percolation ratio (-)	0.28	0.1	0.3	0.08	0.27
Clay	Percolation rate 1m (mm/day)	3.34	0.4	3.49	0.23	2.22
	Percolation rate 2m (mm/day)	2.74	0.11	3.4	0.21	1.74
	Percolation rate 3m (mm/day)	2.13	0.08	3.22	0.19	1.35
	Percolation rate 4m (mm/day)	1.45	0.08	2.48	0.15	0.7
	Percolation rate 5m (mm/day)	1.08	0.08	1.71	0.13	0.15
	Percolation ratio (-)	0.16	0.08	0.23	0.07	0.04

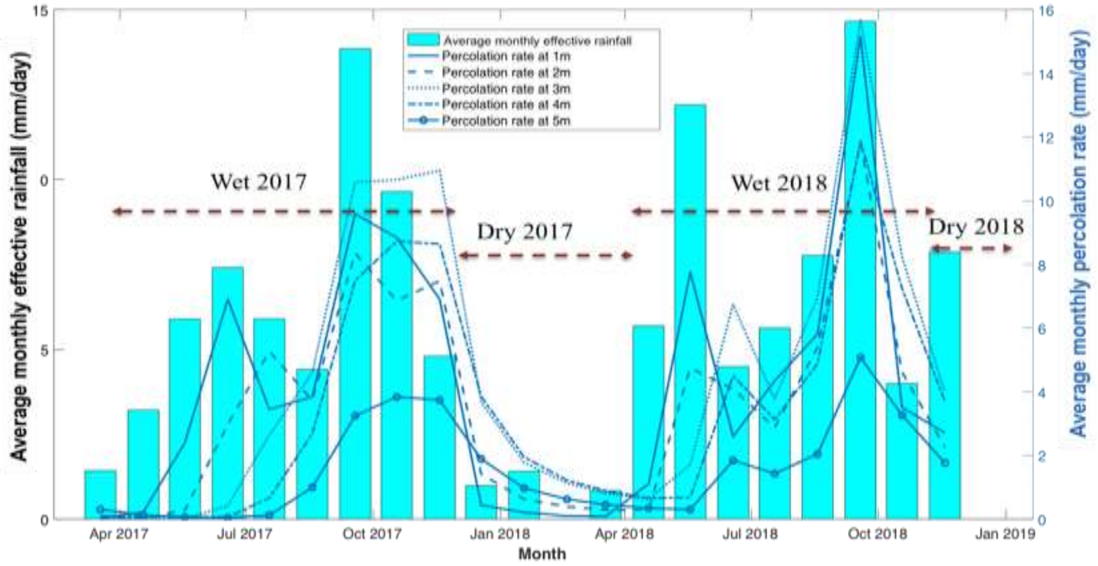

Figure 8 Average monthly percolation rate of sand clay and effective rainfall

The percolation fluxes were compared with effective rainfall to find the percolation rate function of the study area. Figure 9a demonstrates percolation rate function with average monthly effective rainfall. The highest percolation rate is sand clay loam and the lowest is clay. The deep percolation rates are affected from rainfall intensity. Under rainfall intensity 4-14mm/day, the average monthly percolation rate of sand clay loam, sand clay, and clay are in range 2-4.5 mm/day, 1.5-3.5 mm/day, and 0.5-2 mm/day, respectively. Besides, this experiment also reveals that grain size of soil and percentage of sand has strong relationship with percolation flux in wet period (as shown in Figure 8 and 9b), i.e., the higher sand percentage gives higher percolation rate.

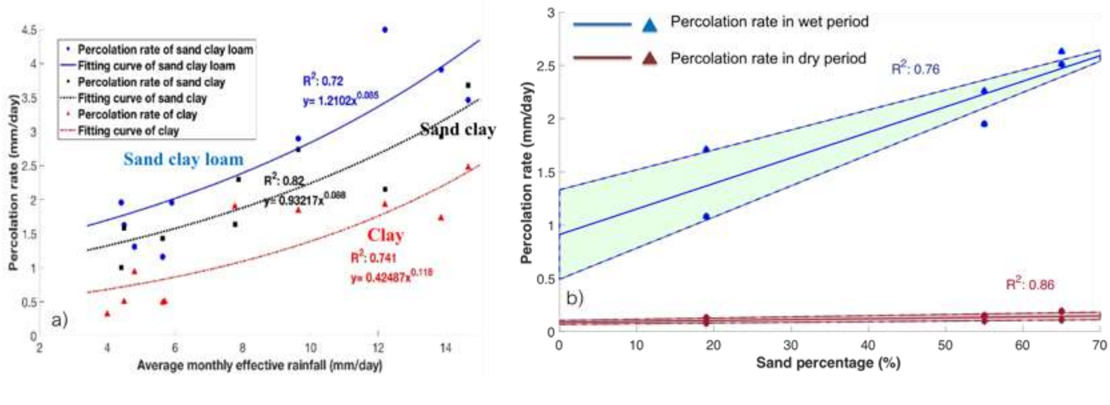

Figure 9 Percolation functions of soil types and in the wet and dry periods

4. CONCLUSIONS

The field sensor measurement system was successfully installed in three locations in the Saigon Basin, Vietnam and the daily deep percolation of 3 soil types (sand clay loam, sand clay, clay) were analyzed by using the Hydrus 1D model calibrated by the daily field experimental data from Oct 2017- Dec 2018 in the study area.

The average monthly percolation rates of three soil type pattern correspond to effective rainfall, rainfall intensity and soil type. The deep percolation proceeds mainly in wet period, while dry period gave very low percolation (as an example in Figure 8). The percolation rate at 5 meter depth is in range 0-4 mm/day. Average percolation rates of three soil type are analyzed in dry and wet periods of Apr 2017-Dec 2018. Due to the permeability property of soil, the derived percolation rate in fluxes in deeper depth are lower than in upper depth of each soil type in the study area. The percolation is the highest for sand clay loam and the lowest for clay. The average monthly percolation rate of sand clay loam, sand clay, and clay varies 2-4.5 mm/day, 1.5-3.5 mm/day, and 0.5-2 mm/day, respectively to rainfall intensity 4-14mm/day. Besides, grain size of soil and percentage of sand has strong relationship with percolation flux in wet period, i.e., the higher sand percentage gives higher percolation rate.

This experiment presented an insights approach to estimate better deep percolation from effective rainfall via field soil moisture sensor system. The approach assisted to give better understanding relationships of deep percolation with effective rainfall, rainfall intensity and soil type. The experiment gave an insight on deeper percolation characteristics as well as potential land recharge from rainfall utilizing soil moisture approach for future groundwater balance evaluation.

ACKNOWLEDGEMENTS

This paper could not be accomplished without the support of Ph. D sandwich program scholarship from AUN – Seed net and the Water Resources System Research Unit of Faculty of Engineering, Chulalongkorn University. The authors also thank to the staff at Division for Water Resources Planning and Investigation for the South of Vietnam, Southern Regional Hydrometeorology Center Department of Resources and Environmental for data collection.

REFERENCES

[1] Koontanakulvong S., and Siriputtichaikul P., Groundwater Modeling In the North Part of the Lower Central Plain, Thailand. in International Conference On Water and Environment, Bhopal, India, Vol. Ground Water Pollution. 2003.

[2] Tran Thanh Long and Koontanakulvong Sucharit. Groundwater and River Interaction Impact to Aquifer System in Saigon River Basin, Vietnam. under submitted to Engineering Journal, 2019.

[3] Reddy, S.J., A simple method of estimating the soil water balance. Agricultural Meteorology, 1983. 28(1): p. 1-17.

[4] Lal, R. Current research on crop water balance and implications for the future. Proceedings of the International Workshop of the Soil Water Balance in the Sudano-Sahelian Zone, Niamey, Niger. 1991.

[5] Kumar, C., Estimation of natural ground water recharge. ISH Journal of hydraulic Engineering, 1997. 3(1): p. 61-74.

[6] Feltrin, R.M., et al., Lysimeter soil water balance evaluation for an experiment developed in the Southern Brazilian Atlantic Forest region. Hydrological Processes, 2011. 25(15): p. 2321-2328.

[7] Tsujimura, M., et al., Behavior of subsurface water revealed by stable isotope and tensiometric observation in the Tibetan Plateau. Journal of the Meteorological Society of Japan. Ser. II, 2001. 79(1B): p. 599-605.

[8] Khalil, M., et al., Analysis of zero flux plane behavior under periodical water supply. Transactions of the Japanese Society of Irrigation, Drainage and Reclamation Engineering, Japan, 2006.

[9] Yeh, H.-F., et al., Estimation of groundwater recharge using water balance model. Water Resources, 2007. 34(2): p. 153-162.

[10] Cao, G., Recharge estimation and sustainability assessment of groundwater resources in the North China Plain. 2011: The University of Alabama.

[11] Feiznia, S., M. Kholghi, and A. Malekian, Groundwater recharge simulation using a coupled saturated-unsaturated flow model. Journal of Applied Hydrology, 2014. 1(2): p. 1-9.

[12] Wu, J. and R. Zhang. Analysis of rainfall infiltration recharge to groundwater. in Proceedings of Fourteenth Annual American Geophysical Union: Hydrology Days. 1994.

[13] Sangbun, W., S. Sangchan, and P. Mekpruksawong, Groundwater Recharge in the Irrigated Upstream Area of the Regulating Gate in the Lower Nam Kam River, Thailand. The 9th International Symposium on Social Management Systems SSMS2013, 2-4 December 2013, Sydney, Australia, 2014. Vol.1 (Issue 9).

[14] Khai, H.Q. and Koontanakulvong S., Impact of Climate Change on groundwater recharge in Ho Chi Minh City Area, Vietnam. in Int. Conf. on Climate Change and Water & Environment Management in Monsoon Asia, Bangkok, Thailand. 2015, Chulalongkorn University.

[15] Koontanakulvong S. and Suthidhummajit C., “The role of groundwater to mitigate the drought and as an adaptation to climate change in the Phitsanulok Irrigation Project, in the Nan Basin, Thailand,” Jurnal Teknologi (Sciences & Engineering), vol. 76, no.15, p. 89–95, 2015.

[16] Tuan, P.V. and Koontanakulvong S., Groundwater and River Interaction Parameter Estimation in Saigon River, Vietnam. Engineering Journal, 2018. 22(1): p. 257-267.

[17] Lutz, A., et al., Fluctuation of groundwater levels and recharge patterns in Northern Ghana. Climate, 2014. 3(1): p. 1-15.

[18] Hung Vu, V. and B.J. Merkel, Estimating groundwater recharge for Hanoi, Vietnam. Science of The Total Environment, 2019. 651: p. 1047-1057.

[19] Seiler, K., Isotope studies of the hydrological impact of large scale agriculture, in Isotope techniques in the study of environmental change. 1998.

[20] Moser, H. and W. Rauert, Isotopic tracers for obtaining hydrologic parameters, in Isotopes in the Water Cycle. 2005, Springer. p. 11-24.

[21] Kojima, Y., et al., Low-Cost Soil Moisture Profile Probe Using Thin-Film Capacitors and a Capacitive Touch Sensor. Sensors, 2016. 16(8): p. 1292.

[22] Simunek, J., M.T. Van Genuchten, and M. Sejna, The HYDRUS-1D software package for simulating the one-dimensional movement of water, heat, and multiple solutes in variably-saturated media. University of California-Riverside Research Reports, 2005. 3: p. 1-240.

[23] Schaap, M.G., F.J. Leij, and M.T. Van Genuchten, Rosetta: A computer program for estimating soil hydraulic parameters with hierarchical pedotransfer functions. Journal of hydrology, 2001. 251(3-4): p. 163-176.

[24] Yang, H., et al., Factors affecting drying and wetting soil-water characteristic curves of sandy soils. 2004. 41(5): p. 908-920.

[25] Pwint Phyu Aye, Koontanakulvong S., and Tran Thanh Long, Deep Percolation Characteristics Via Field Soil Moisture Sensors – Case Study in Phitsanulok, Thailand –. Taiwan Water Conservancy, 2019. Vol. 67, No. 1.

[26] Kangboonma, N. and Koontanakulvong S., Deep Percolation Characteristics via Field Moisture Sensor Measurements in Rice Experimental Field, Phitsanulok, Thailand, Int. Conf. on Climate Change and Water & Environment Management in Monsoon Asia, Bangkok, Thailand. 2019, Chulalongkorn University.